Bimolecular recombination in polymer electronic devices

C. Groves* and N. C. Greenham
Optoelectronics Group, Cavendish Laboratory, Cambridge, CB3 OHE, United Kingdom
(Received 15 July 2008; published 28 October 2008)

We investigate the rate constant for Langevin-type bimolecular recombination using a Monte Carlo model. It is found that filamentary transport, mobility anisotropy, restriction of transport in one dimension, and confinement of electrons and holes to one transporting component within a blend can cause significant deviations from classical Langevin behavior. We discuss in detail the reasons for the failure of the Langevin model for these instances, provide alternative formula, and comment upon the implications for polymer transistors, LEDs, and photovoltaics.

DOI: 10.1103/PhysRevB.78.155205 PACS number(s): 72.10.Bg, 72.20.Jv, 72.80.Le, 73.61.Ph

I. INTRODUCTION

Bimolecular recombination of charge carriers is of fundamental importance for a wide range of polymer electronic devices. Significantly, it is the process that provides light emission in ambipolar light-emitting field-effect transistors (LFETs) and light-emitting diodes (LEDs). Its effects are also important in photovoltaic (PV) devices although deleterious in this instance, as it limits fill factor under solar illumination and gives rise to sublinear intensity dependence of the photocurrent. Clearly it is important that we have good understanding of the processes leading to bimolecular recombination and the mathematical tools to describe them. As we discuss below, most attempts to quantify bimolecular recombination in these polymer devices fail to a large extent. In this paper we show that these failures are primarily because the context in which transport occurs, for example, the quasi-two-dimensional (2D) nature of transport in LFETs is not taken into account. By taking into account the context we explain a wide range of discrepancies between experiment and theory in these technologically important devices while also presenting alternative equations appropriate to these instances.

The total rate of bimolecular recombination in a device can conveniently be considered as being due to two sequential processes. First, there is the rate at which a pair of carriers within a random ensemble are transported toward one another. The rate constant for this process is defined as β, which is normalized in units of carrier density for electrons and holes, n and p, respectively, such that the total rate at which carriers meet per unit volume is βnp. Second, there is the efficiency with which a pair of carriers in close proximity recombine, η, which is determined by the competition of the hopping rate with the recombination rate for adjacent carriers. Since the mean-free path in a polymer λ ($\sim$1 nm) is typically much smaller than the thermal capture radius, r_c ($\sim$20 nm at room temperature), transport will comprise many hops. In this regime the Langevin expression[1] is typically used to describe the rate constant,

$$\beta = \frac{q(\mu_e + \mu_h)}{\varepsilon \varepsilon_0}, \tag{1}$$

where q is the electronic charge, μ_e and μ_h are the electron and hole mobilities, ε_0 is the permittivity of free space, and ε is the relative permittivity. Although bimolecular recombination is generally transport controlled in polymers, it is worth remembering that there are a range of other implicit assumptions inherent in Eq. (1) that are not satisfied in real devices. In particular, electrons and holes are assumed to be distributed uniformly, which is violated in materials with a large degree of energetic disorder; the transport is assumed to be in three dimensions, which is violated in multilayer LEDs and LFETs; carriers are assumed to inhabit the same homogeneous medium, which is violated in blend and bilayer PVs, and multilayer LEDs; finally, transport is assumed to be isotropic, which may be violated in materials with a high degree of ordering. Despite these inadequacies, the use of Eq. (1) in these various regimes is widespread. It is therefore not surprising that the agreement between experiment and theoretical predictions, underpinned by Eq. (1), is frequently poor.

In homogeneous materials it is expected that η will approach unity, and so the rate of bimolecular recombination is described completely by β. Thus homogeneous materials provide a very useful experimental avenue to test the validity of Eq. (1). In simple molecular crystals, Eq. (1) is shown to work very well.[2,3] This however seems to be the exception rather than the rule for polymer devices. For example, Blom *et al.*[4] used a simple analytical technique to show the effective recombination rate constant $\beta_{\text{eff}} \sim 4\beta$ in poly(dialkoxy *p*-phenylene vinylene) (PPV) LEDs. More recently, ambipolar LFETs, in which transport is confined to an accumulation layer of $\sim$1 nm, have allowed more direct inspection of recombination behavior in homogeneous films.[5] In this more complicated structure, the agreement between Eq. (1) and experiment is even worse as the predicted recombination zone width of $\sim$0.5 μm in poly(9,9-dioctylfluorene-*co*-benzothiadiazole) (F8BT) and poly{(9,9-dioctylfluorene)-2,7-diyl-alt-[4,7-bis(3-hexylthien-5-yl)-2,1, 3-benzothiadiazole]-2′2″ diyl} (F8TBT) LFETs is significantly less than the measured widths of 2–4 μm.[6] Similarly poor agreement between measured and predicted recombination behaviors has been demonstrated in LFETs fabricated from other polymers as well.[7] Still greater deviations from the Langevin equation occur in materials which have anisotropic carrier mobility as Zaumseil *et al.*[8] have shown that LFETs fabricated from aligned F8BT have β_{eff} that is three orders of magnitude smaller than that predicted by Eq. (1).

In polymer PVs, electrons and holes are confined to their respective accepting polymers and so the recombination rate

is intrinsically lower than in homogeneous films; consequently recombination competes with hopping in such devices and $\eta < 1$. This makes determination of the recombination rate constant in polymer PVs challenging since the recombination rate is determined both by the rate constant *and* the recombination efficiency. The recombination efficiency is, however, relatively well-understood courtesy of the analytical model of Onsager,[9] and the later refinement by Braun.[10] Subsequently, a number of Monte Carlo methods[11–15] have additionally clarified the effect of morphology, carrier mobility, and energetic disorder upon η. These papers show that η increases as mobility decreases, which is counter to the mobility dependence of β. This would suggest that, if the measured recombination rate increased with increasing mobility, we may be probing the rate constant. That said, given the interconnected nature of the transport and recombination processes,[16] it seems a challenging prospect to ensure that one has deconvolved completely the effects of β and η from experimental data. Pivrikas *et al.*[17] used a time-of-flight technique to measure the recombination rate and the mobility simultaneously in an annealed poly(3-hexylthiophene) (P3HT): 1-(3-methoxycarbonyl) propyl-1-phenyl-[6,6]-methanofullerene (PCBM) blend PV device and found that the time dependence of mobility matched that of the recombination rate, suggesting that the observed recombination behavior was due to the rate constant. This experiment found $\beta_{\text{eff}} \sim 10^{-3}\beta$, which has been supported by additional time-of-flight,[18,19] photo-CELIV,[18,20] and double-carrier injection[20,21] measurements on similar devices. These findings are in quantitative agreement with those of the Groningen[22] and Imperial College[23] groups who used different techniques to quantify β_{eff}/β on annealed P3HT:PCBM blend devices. However, not all blend devices show the same dramatic deviations from the Langevin equation as seen in annealed P3HT:PCBM devices, for example, poly[2-methoxyl-5-(3,7-dimethyloctyloxy)-phenylene-vinylene] (MDMO-PPV):PCBM blends have $\beta_{\text{eff}}/\beta \sim 0.5$.[24] Therefore, it seems to be the case that blends are characterized by sub-Langevin recombination rates but the extent to which the Langevin expression overestimates the rate constant depends upon the materials and processing conditions. These data have further significance, as while the rate constant in blends is sub-Langevin, it has shown that bimolecular recombination is still of Langevin type, i.e., that recombination is limited by mobility. This suggests that the intrinsic mechanism of transport-controlled recombination needs to be modified rather than replaced.

Thus there is a large amount of evidence that the rate constant deviates significantly from the Langevin expression in a number of technologically important devices. We therefore need to understand why the Langevin expression is deficient in these cases and to provide an alternative. The differences between theory and experiment in LFETs may be due to the near two-dimensional transport in these devices. Greenham and Bobbert[25] showed by using a variety of techniques that in the limit of two-dimensional transport the rate constant becomes weakly dependent upon charge density but did not relate this to the expectations of the Langevin expression. In LFETs and multilayer LEDs it seems likely that carriers will be confined to within a few nanometers of an interface, and so the rate constant may not be described well by either the three-dimensional limit described by Langevin or the two-dimensional limit described by Greenham and Bobbert.[25] For devices comprising electron- and hole-accepting polymers, there seems to be a broad consensus from experiment that β_{eff} is smaller than that predicted by the Langevin expression. However, the mechanism for this modification is not commonly agreed upon and has variously been attributed to the spatial separation of carriers,[26] trapping via energetic disorder,[27] or isolated deep states,[28] and the slower carrier's transit to the heterointerface being the rate-limiting step.[22] While these mechanisms are physically plausible, there is no comparative study of these effects to enable consensus on the issue. A number of Monte Carlo simulations[29–31] have been used to clarify various aspects of recombination behavior. However, these studies either report recombination cross sections rather than the rate constants demanded for macroscopic drift-diffusion modeling or do not calculate the rate constant directly. Preliminary modeling by the authors in Ref. 8 has shown for a limited set of circumstances the effect of anisotropy and dimensionality upon the rate constant. Here we extend this work to reveal general trends, and thus explain the differences between experimental data and the predictions of the Langevin expression and experiment. To do this we use a Monte Carlo model that can evaluate β_{eff} directly, and use this to characterize the effect of mobility anisotropy, dimensionality, and the restriction of carriers to respective polymer types upon β_{eff}. We present discussions as to why the Langevin expression fails in each case and present alternative analytical formula that can be used in these circumstances.

II. MODEL DETAILS

The simulation volume comprises of a cubic regular lattice of hopping sites spaced by 1 nm. The size of the simulation volume was varied for each trial to safeguard against finite-size effects, particularly for large anisotropy ratios. To obtain size-independent rate constants, the volume typically had to be 50–350 nm in extent along each side. Each site is assigned a Gaussian distributed energetic disorder of standard deviation, σ. We assume that there is no correlation between the values of energetic disorder on neighboring sites. This simplifying assumption may not be a good approximation of transport for all polymer devices but seems to give reasonable agreement with measured experimental data for PVs.[11] We assume that energetic disorder will affect the energy for an electron and hole in the same manner. Since hopping transport in disordered media has recently been shown to be filamentary in nature,[32] this assumption implies that electrons and holes preferentially follow the same filaments. Electrons and holes are injected at random unoccupied positions within the lattice until a chosen charge density is reached. All simulations in this paper have $n=p$. Hopping rates from the current site i to a nearest-neighbor site j are calculated by a Marcus rate expression,[33]

$$R_{i\to j} = \upsilon_{\text{hop}} \times \exp\left(-\frac{(E_j - E_i + E_R)^2}{4E_R kT}\right). \tag{2}$$

Here E_i and E_j are the potential energies of the sites i and j, respectively, E_R is half the polaron energy, and υ_{hop} is a prefactor which quantifies the wave-function overlap between neighboring highest occupied molecular orbital (HOMO) or lowest unoccupied molecular orbital (LUMO) levels. The energies used in Eq. (2) include energetic disorder, applied electric field, F, and Coulomb interactions between carriers up to the thermal capture radius, which here is 21 nm ($\varepsilon=3$). Cyclic boundary conditions are allowed for hopping and for the Coulomb potential in all directions. The simulation volume is chosen to be larger than the Coulomb interaction radius to avoid self-interaction of carriers. Of all possible options, the one with the shortest waiting time is chosen as the behavior for that carrier before being entered into an appropriate place in the queue. After each event, the potential landscape upon which the hopping rates depend will alter. Hence, in order to ensure that the hopping rates of carriers are always appropriate to its surroundings, we recalculate the behavior of each carrier after every hopping or recombination event. This rather computationally expensive method is referred to as the dynamical Monte Carlo method, which contrasts to the more commonly used first reaction method,[34] in which the behavior of an individual carrier is calculated only once immediately after it has completed its previous hop. Previous comparisons between these two methods for smaller charge densities than those examined here have shown little difference,[11] and indeed we presently find that there is little discernible difference between the two methods for homogeneous materials with isotropic mobility. However, since over the course of this paper we will be examining a great many physical cases, we err on the side of caution and use the more correct dynamical Monte Carlo method.

Recombination occurs between adjacent dissimilar carriers instantaneously, and therefore our recombination rate quantifies the rate constant, β_{eff}. When a pair of carriers recombine, they are removed from the simulation, whereupon we inject a replacement electron and hole at random unoccupied positions. This continues until the xth recombination event occurs, upon which the simulation is stopped and the time t_x is noted. The simulation is repeated many times with different configurations of energetic disorder and initial carrier positions to determine $\langle t_x \rangle$ reliably. The process of averaging over many recombination events is necessary since it lessens the importance of the carrier start positions. For each simulation the value of x is increased until the average inter-recombination time becomes independent of x, which for most simulations reported here occurs for $x \sim 300$.

If we are to make comparisons between the measured β_{eff} and the Langevin-predicted β, we must also know the mobility of the charge carriers for the given charge density. Thus we use two simulations: one to predict the mobility and one to predict the recombination dynamics, which have the same transport parameters. To measure the mobility, only one carrier type is injected, a field is applied, and then the average distance traveled downfield is measured for a given length of time. When energetic disorder is present, we allow the carriers sufficient time to settle in the density of states before measuring the equilibrium mobility. This poses a problem for the model of recombination dynamics, as if we were to inject carriers at random positions within a lattice with uncorrelated disorder, their energy distribution would match the density of states. Albrecht and Bässler[15] have shown that, in the low charge-density limit, carriers relax to have an energy distribution with mean energy $-\sigma^2/kT$ and standard deviation σ. Thus, injecting carriers at random gives carriers a nonequilibrium energy distribution, which in turn enhances their mobility over short time scales. We expect for real devices that thermalization will be rapid, and so carriers will have an energy which is closer to the quasi-Fermi level than the center of the density of states. To resolve this problem for the recombination dynamics model, the energetic disorder for each site upon which a carrier is "injected" is rechosen from the equilibrium energy distribution. In this way, the short-time mobility of the carriers is the same as the equilibrium mobility which we measure directly using the Monte Carlo mobility model described above. Obviously this method distorts the energetic disorder distribution to an extent that increases with charge density. However, we anticipate this effect to be small since the peak charge density considered (5×10^{17} cm^{-3}) corresponds to only 0.1% of the hopping sites, having their energetic disorder picked from the equilibrium energy distribution. When a carrier recombines, we rechoose the disorder for the injection site of the recombined carrier from the density of states and rechoose the disorder of the injection site for the replacement carrier from the equilibrium energy distribution. In this way the number of sites with disorder that is not picked from the density of states stays constant throughout the simulation.

TABLE I. Parameters used in the simulation.

Disorder (meV)	υ_{hop} (s^{-1})	E_R (J)	T (K)	ε
0	4×10^{11}	1.2×10^{-19}	298	3
75	9.5×10^{12}			
100	1.8×10^{14}			

In the following simulations we use three sets of parameters corresponding to $\sigma=0$, 75, and 100 meV. The remaining parameters, shown in Table I, are chosen to be physically reasonable and to give steady-state mobility of 10^{-4} cm^2/V s when $F=10^7$ V/m unless otherwise stated. Mobility varies linearly with υ_{hop} and thus the mobility is changed along appropriate axes by scaling υ_{hop} by the appropriate amount. For the homogeneous materials, electrons and holes are allowed to occupy any unoccupied hopping site, whereas carriers are restricted to their own polymer type in blend electron- and hole-transporting material. A blend morphology of average feature size $d=4$ nm was generated by a process of simulated annealing in the same manner as in Ref. 11. Blend morphologies with coarser feature sizes were made by an approximate technique in which a 4 nm blend is simply scaled by a factor.[35] Quasi-two-dimensional structures were realized by removing cyclic boundary conditions in one dimension, and in limiting the extent of the simulation volume to an extent l.

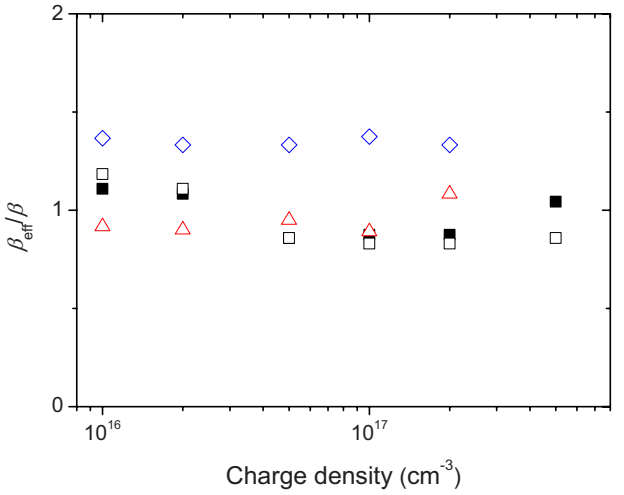

FIG. 1. (Color online) β_{eff}/β as a function of charge density, $n=p$. Squares correspond to $\sigma=0$, triangles to $\sigma=75$ meV, and diamonds to $\sigma=100$ meV. Open symbols represent $F=0$ and closed symbols represent $F=10^7$ V/m.

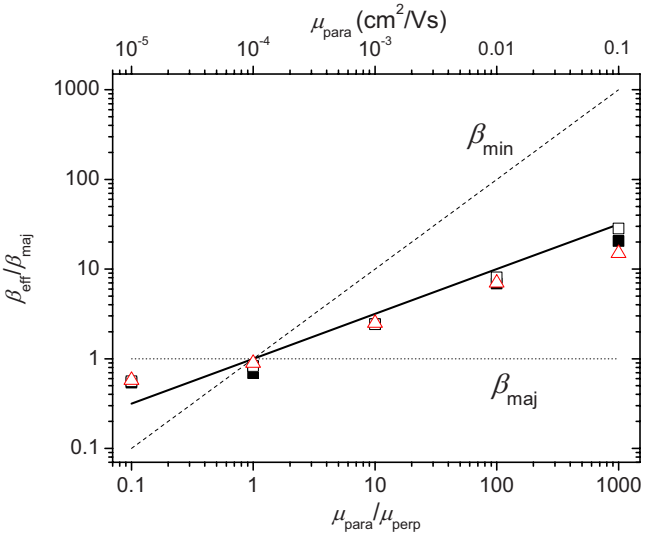

FIG. 2. (Color online) Measured β_{eff} normalized to the Langevin prediction of the transport rate using the major axis mobility, β_{maj}. Squares correspond to $\sigma=0$ and triangles to $\sigma=75$ meV. Open symbols represent $F=0$ and closed symbols represent $F=10^7$ V/m. The dashed lines show the predictions of the Langevin equation using either the major or minor axis mobility while the solid line shows the predictions of Eq. (3).

III. HOMOGENEOUS MATERIALS

A. Materials with isotropic and anisotropic mobilities in the bulk

Our first experiment is to test the equivalence of β_{eff} with β for the simple case of homogeneous material with isotropic mobility. Figure 1 shows β_{eff}/β for charge densities of 10^{16} cm$^{-3} \leq n=p \leq 5\times10^{17}$ cm^{-3}, fields of 0 V m$^{-1} \leq F \leq 10^7$ V m^{-1}, and energetic disorder of 0 meV $\leq \sigma \leq 100$ meV, representing a typical range of conditions one might find within polymer devices of varying types. Over the range $0 \leq \sigma \leq 75$ meV, the Langevin result is reproduced ($\beta_{eff}/\beta \sim 1$). However, for $\sigma=100$ meV we find that the rate constant is enhanced, compared to the Langevin prediction, by ~35%. This is very likely to be a consequence of filamentary transport. Energetic disorder naturally divides up the transporting medium into regions through which transport is more or less energetically favored, the former being called a filament.[32] The efficacy of disorder in forming filaments depends upon the relative magnitudes of σ and kT. If σ is small compared to kT, the "guiding" effect of disorder is weak and so transport more closely approximates the assumption of homogeneous transport upon which the Langevin equation is based. When σ is large compared to kT, carriers are increasingly localized within the filamentary regions, and thus bimolecular recombination is faster for a given charge density.

To examine the effects of mobility anisotropy, we define a single axis, hereafter the minor axis, upon which the mobility, μ_{min}, is varied. The other two, hereafter major, axes have a constant mobility, μ_{maj}. In Fig. 2 we show the effect of altering μ_{min} upon the rate constant, normalized to the prediction of the Langevin equation using the mobility μ_{maj}, β_{maj}. To aid in the interpretation, we also show the predictions of the Langevin equation for an isotropic system with mobility μ_{maj} (β_{maj}) and also for μ_{min} (β_{min}). Unsurprisingly we find the predicted rate constants for an anisotropic system comprising mobilities μ_{maj} and μ_{min} between those of isotropic systems with mobilities μ_{maj} and μ_{min}. Consequently the Langevin equation using either μ_{maj} or μ_{min} becomes an increasingly poor predictor of the rate constant as mobility anisotropy increases (although it would perhaps be unfair to assert that the expression has failed since it is being used far outside the founding assumptions upon which it is based). We find that for the case of equal, anisotropic electron and hole mobilities, the rate constant can be fitted very well by the following

$$\beta_{aniso} = \frac{2q\sqrt{\mu_{maj}\mu_{min}}}{\varepsilon\varepsilon_0}. \tag{3}$$

The predictions of Eq. (3), also shown in Fig. 2, are in good agreement with the Monte Carlo data over four orders of magnitude of mobility anisotropy. Note that we do not report data below $\mu_{min}/\mu_{maj} < 0.1$ since it was beyond the memory capacity of our computer system to have a simulation volume sufficiently large to ensure accurate data. In the limit of zero mobility along the minor axis, we reproduce, approximately, the two-dimensional limit which will be discussed in Sec. III B.

It should be noted that the mobility, and any associated anisotropy, alters with length scale for a real polymer device. Practically we expect mobility anisotropy to occur due to the intentional alignment of polymer chains, as in Ref. 8, or by spontaneous organization of polymer chains into crystalline domains. Thus on the length scale of the thermal capture radius, which is important in determining whether a charge pair will recombine, the transport will be characterized by fast intrachain hops down the chain length of ~10 nm and a significant mobility anisotropy. On the length scale of a device, however, the macroscopic drift mobility along the

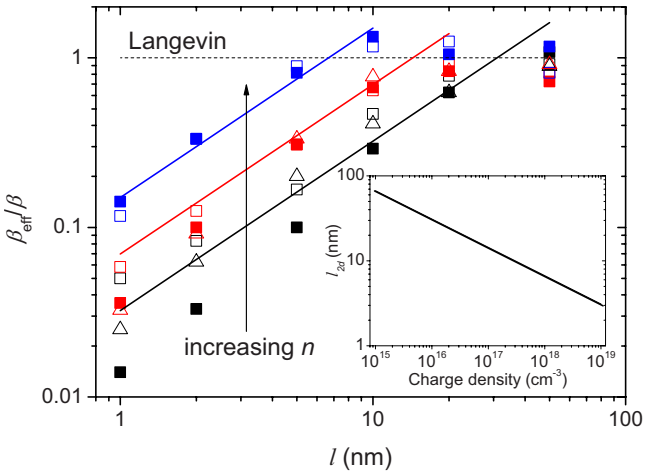

FIG. 3. (Color online) $\beta_{\mathrm{eff}}/\beta$ as a function of the simulation volume extent in one dimension, l. $l=1$ nm corresponds to the 2D limit. Open symbols correspond to $F=0$ while closed symbols to $F=10^7$ V/m (which is in the plane of the confined layer). We show data for $\sigma=0$ meV (squares) and $\sigma=75$ meV (triangles), when the charge density is $n=p=10^{16}$ cm^{-3} (black), 10^{17} cm^{-3} (red), and 10^{18} cm^{-3} (blue). In all cases the isotropic mobility is 10^{-4} cm^2/V s. The dotted line corresponds to the prediction of the Langevin relation, while the solid lines show the predictions of Eq. (4) for the charge densities examined. The inset shows the volume thickness below, in which two-dimensional transport is expected from Eq. (5).

alignment direction will be limited by interchain hops. Consequently, the drift mobility anisotropy will be smaller than that on the nanoscopic scale. Including the nanoscopic detail of the finite polymer chain lengths is beyond the scope of this paper but will be important to study in the future.

B. Effect of constraining transport in one dimension

Greenham and Bobbert[25] have shown that bimolecular recombination in the two-dimensional limit can only be described by second-order kinetics if β is allowed to vary as $n^{0.43}$, in contrast to the density-independent rate constant found in three dimensions by Langevin.[1] Here we characterize the transport behavior in the transition between two and three dimensions, a regime which most closely corresponds to LFETs and multilayer LEDs. Figure 3 shows $\beta_{\mathrm{eff}}/\beta$ for $1\ \mathrm{nm} \leq l \leq 50$ nm and a variety of charge densities. At large l the values of β_{eff} agree with those measured in the bulk shown in Fig. 1. As l reduces, $\beta_{\mathrm{eff}}/\beta$ begins to fall simply because the intercarrier spacing for a given charge density increases as transport in one dimension is increasingly constrained, leading to a correspondingly smaller β_{eff}. In the two-dimensional limit (here this is $l=1$ nm) $\beta_{\mathrm{eff}}/\beta$ is less than unity by a factor that is dependent upon the concentration. Hence, we recreate the result in Ref. 25, i.e., that two-dimensional transport gives rise to a weak dependence of β_{eff} on n. What is interesting to note is that this two-dimensional behavior (i.e., $\beta_{\mathrm{eff}}/\beta < 1$ and β_{eff} varying with n) can occur for relatively weak confinement. The factor change in rate constant with respect to the prediction of the Langevin equation ($=\beta_{\mathrm{eff}}/\beta$) can be fitted very well by

$$\gamma = 1.5 n^{1/3} l. \tag{4}$$

We show the predictions of Eq. 4 in Fig. 3, which can be seen to be good over a wide range in charge density and l. This expression is in reasonable agreement with the findings of Greenham and Bobbert,[25] who found that the rate constant was proportional to $n^{0.43}$ in the limit of two-dimensional transport. Equation (4) is valid in the regime where $\gamma < 1$, which interestingly corresponds to the range where the spacing between carriers in a three-dimensional volume for a given charge density is similar to, or larger than, l. Conveniently, setting $\gamma=1$ allows us to define a confinement layer thickness below which there will be two-dimensional behavior,

$$l_{2\mathrm{D}} = \frac{1}{1.5 n^{1/3}}. \tag{5}$$

The inset to Fig. 3 shows the prediction of the boundary for two-dimensional transport given by Eq. (5). It is striking that for the entire range of charge density typically found in the recombination zone of an LFET (10^{16} cm$^{-3} < n,p < 10^{18}$ cm^{-3}), $l_{2\mathrm{D}}$ is substantially in excess of the accumulation layer thickness of ~ 1 nm.[36] It therefore seems likely that LFETs *generally* operate in the two-dimensional transport regime, which is characterized by a rate constant that is both reduced below the bulk value and weakly charge-density dependent.[25] This may explain, or at least play some role, in the general failings of drift-diffusion modeling to reproduce correctly the size of recombination zone in LFETs. This is supported by estimates of recombination zone width being typically too small.[6,7] Taking a specific example, the recombination zone in F8BT is predicted to be ~ 0.5 μm which compares to the measured values of 2–4 μm.[6] Making reasonable estimates of an accumulation layer thickness of 1 nm, and $n=p=10^{17}$ cm^{-3} in the recombination zone [Eq. (4)] predicts $\gamma=0.069$. The analytical technique in Ref. 37 predicts that this reduction in the rate constant would result in a widening of the recombination zone by a factor ~ 3.8, much improving upon the fits using the standard Langevin expression. The current result also has bearing upon the performance of multilayer LEDs as Eq. (4) and Ref. 25 show that the light output of these devices should scale superlinearly with mobilities of the electron- and hole-transporting media. When applying these results to multilayer LEDs, one should remember that it does not consider the possibility of hopping over the heterointerface, which is likely to reduce the effect confinement for small potential barrier heights. A discussion of these issues is presented in Ref. 38.

Now that we have characterized the effect of anisotropy and confinement upon the recombination behavior, we discuss the wider implications of these results in LFETs. The LFET architecture provides a possible candidate for electrically pumped organic lasers due to the high current density. However, in a recent paper, Naber *et al.*[39] have predicted that such devices are some three orders of magnitude of current density below that required for lasing. As we have seen, alignment of the polymer chains significantly alters both the transport and recombination behaviors, and so may provide a

promising route to realizing an electrically pumped organic laser. The crucial quantity we wish to maximize is the exciton density, which scales as I/W, where I is the drain current and the W is the width of recombination zone. The current is determined by the macroscopic drift mobility in the direction of current flow, which can be improved by aligning the polymer chains along the channel. For an isotropic mobility, W is predicted to be independent of mobility since it is determined by a balance between transport and recombination rates.[37] However, for an aligned system we have shown above that the recombination rate will be significantly reduced due to the contribution from $\mu_{\min}$, causing an increase in W which will counteract the improvement in I.[40] Indeed, alignment of polymer chains in F8BT LFETs resulted in an increase in I by a factor of only ~ 3 whereas W increased by a factor of ~ 10, actually reducing the exciton density in this case.[8] It therefore seems unlikely that polymer chain alignment could provide the improvement in exciton density necessary to realize an electrically pumped polymer laser.

IV. ELECTRON- AND HOLE-TRANSPORTING MEDIA

The most comprehensive set of experimental evidence for deviations of the recombination behavior from the Langevin equation comes from donor-acceptor systems. These deviations are significant in annealed P3HT:PCBM solar cells, with the rate constant being three orders of magnitude smaller than the predictions of the Langevin equation. In other blend systems the rate constant is also smaller than the prediction of Langevin but only by a factor of less than 10. In this section we use the Monte Carlo model to examine the effect of constraining electrons and holes to their respective polymers upon the rate constant in an attempt to explain these data.

Figure 4 shows measured β_{eff} values for 1:1 blends with average domain sizes d of 4 and 35 nm. First we shall discuss the morphology with $d=4$ nm. When the mobilities are equal, we find that $\beta_{\text{eff}} \sim 0.5\beta$, in contrast to homogeneous material where isotropic, equal mobilities for electrons and holes gave $\beta_{\text{eff}} \sim \beta$. This is because carriers must travel to the interface in order to recombine and, on average, one of the carriers is likely to be stuck at the interface while the other carrier completes its longer trajectory, in a similar manner to that described in Ref. 22. Thus the factor 0.5 represents the effect of having one carrier "wait" at the interface averaged over many different starting positions of electrons and holes on either side of the interface. When the electron mobility is varied, β_{eff} varies in a manner that is mostly sympathetic to the Langevin equation. We do however find that $\beta_{\text{eff}} \sim 0.2\beta$ for a mobility ratio of three orders of magnitude, in comparison with $\beta_{\text{eff}} \sim 0.5\beta$ for equal mobilities, showing that the rate constant has a slight dependence upon the smallest mobility. It was suggested by Koster *et al.*[22] that rate constant was proportional to the smallest mobility and showed that better fits to experimental data were achieved when this smaller rate constant was used for annealed P3HT:PCBM PVs. While we see a slight dependence of the rate constant upon the smallest of the electron and hole mobilities, its effects are not strong, as shown in Fig. 4, for a wide range of morphologies. It is puzzling that the mechanism described in Ref. 22 is not strong since the physical picture seems quite clear. The key to understanding this is to realize that one would expect the smallest mobility to determine the rate constant if all of the carriers start at the same distance from an interface. However, in our simulation and in devices in general, carriers are distributed at a range of positions from the interface. Consequently, even if one of the species of carriers is far slower than the other, there will be a population of these slow carriers close to the interface with which the faster carriers can recombine, leading to the weaker dependence of the rate constant upon the smallest carrier mobility than that predicted in Ref. 22.

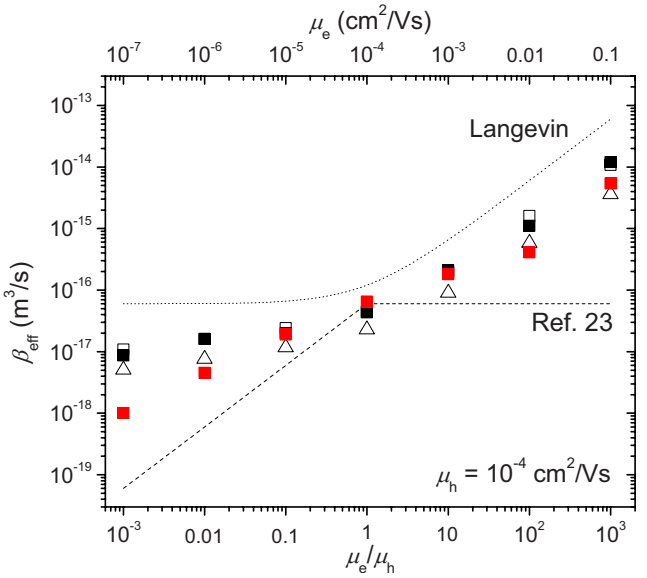

FIG. 4. (Color online) Measured β_{eff} for a 1:1 blend of electron- and hole-accepting polymers with an average feature size of $d=4$ (black) and 35 nm (red). Squares correspond to $\sigma=0$ and triangles correspond to $\sigma=75$ meV. Open symbols represent $F=0$ and closed symbols represent $F=10^7$ V/m. In all cases the isotropic hole mobility is 10^{-4} cm^2/V s. Dotted line shows the prediction of the Langevin equation and the dashed line shows the prediction of Langevin equation when only using the smallest mobility, as suggested in Ref. 23.

Increasing the energetic disorder to 75 meV while keeping the isotropic mobility constant at 10^{-4} cm^2/V s for $d=4$ nm blend is shown to reduce the rate constant over a range of mobility ratios by $\sim 60\%$ compared to the zero disorder case. These results are in contrast to that of homogeneous materials, where increasing the degree of disorder to 75 meV while keeping the isotropic mobility constant at 10^{-4} cm^2/V s made little difference to the rate constant. This is because in a donor-acceptor system we place a restriction upon where recombination can take place (i.e., at the interfaces), and so recombination requires the cooperation of both carriers. Hence, trapping of one carrier at a low-energy site has a larger effect in these systems than in homogeneous systems, where if one carrier traps then the free carrier can traverse the remaining distance and recombine.

The rate constant for the $d=35$ nm blend is smaller than that for the $d=4$ nm blend for the same conditions, and the

reduction is more significant for larger mobility ratios. This is simply because, on average, carriers have to travel further to the interface to recombine in the $d=35$ nm blend than in the $d=4$ nm blend. Making the mobilities more unequal for the larger domain size incurs a longer wait for the more mobile carrier while the slower carrier traverses the large domain, consequently reducing the rate constant. However, this effect is weak, as increasing d by almost an order of magnitude leads to a reduction in the rate constant by a factor of between ~ 1 and ~ 10, depending upon the mobility ratio. Since reported PV devices generally have an optimized domain size ($d \sim 20$ nm) to balance exciton diffusion and geminate pair separation,[35] it seems unlikely that the domain size could be responsible for a reduction in orders of magnitude in the rate constant.

We also examined the effect of an unequal volume fraction of electron- to hole-transporting material, which we do not show. The blend ratio was altered to 8:1 in favor of the electron-transporting material, and an equal number of electrons and holes were injected as previously done. As perhaps might be expected, the rate constant followed much more closely the prediction of the Langevin expression using the electron mobility only. However, this effect is expected not to cause an order-of-magnitude reduction in the rate constant; as in real devices the volume ratio of donor to acceptor material is close to unity to allow continuous pathways for electrons and holes to the contacts. For example, in Ref. 22, which reports $\beta_{\mathrm{eff}}/\beta=10^{-3}$ for an annealed P3HT:PCBM device, the volume fraction of the P3HT to PCBM $\sim 2:3$.

These data can thus explain very well the slight reduction in the rate constant below the Langevin prediction in some donor-acceptor blends[24] through the weak effects of donor-acceptor morphology, mobility mismatch, slight trapping, and unequal volume ratios. However, these mechanisms, as investigated here, are not sufficiently strong to explain the anomalously low rate constant seen in annealed P3HT:PCBM devices. Since we examine the effect of mobility mismatch, domain size, and unequal volume fraction on rate constant over the ranges seen in annealed P3HT:PCBM devices, we can rule out these factors as main contributors to the low rate constant in this case. On this basis, it seems the most likely explanation for the anomalously weak recombination in annealed P3HT:PCBM devices is trapping. While we have showed that weak trapping from energetic disorder with $\sigma=75$ meV causes a slight reduction in the rate constant, deeper traps would have a larger effect. Indeed, this assertion has been made previously by Nelson *et al.*,[28] who showed that one could only fit to the transient photocurrent in P3HT:PCBM solar cells if one included a number of isolated deep traps. One may expect that the rate constant in the presence of trapping would have a concentration dependence, which is seen in experiment.[23] Thus this explanation appears to fit the available data very well. Further work to obtain a quantitative fit of the current model to the rate constant in annealed P3HT:PCBM devices is left to a later paper.

V. CONCLUSIONS

Here we have presented a model that can predict the bimolecular recombination rate constant in a variety of situations appropriate for polymer devices. The Langevin equation is generally found to fail to some extent, other than the case for three-dimensional isotropic transport within materials with energetic disorder of less than 75 meV at room temperature. Increasing the degree of energetic disorder beyond this value increases the rate of recombination due to filamentary transport. Unsurprisingly, mobility anisotropy causes significant deviations from Langevin expression as there is more than one significant mobility to consider. For enhanced mobility along one axis, it is shown that the rate constant is proportional to the square root of the product of the two mobilities in the system. The effect of constraining the transport within one dimension is also examined. It is found the two-dimensional behavior, which is characterized by a reduced rate constant that is charge-density dependent, occurs for relatively weak confinement. This has the implication that light-emitting field-effect transistors generally operate in the two-dimensional regime, perhaps explaining the seemingly constant overestimation of recombination zone width by drift-diffusion models. The effect of constraining the transport of electrons and holes to their respective polymer types, which is important in photovoltaic devices, is also discussed. It is found that donor-acceptor systems do not necessarily lead to large deviations from the Langevin equation, with the effect of domain size, electron-hole mobility mismatch, and energetic disorder reducing the rate constant by less than an order of magnitude. We suggest that the reduced transport rate measured in annealed P3HT:PCBM devices is instead because of deep carrier trapping.

ACKNOWLEDGMENTS

C.G. would like to thank the European projects NAIMO (Contract No. NMP-CT-2004–50035) and MODECOM (Contract No. NMP-CT-2006–016434) for funding. The authors would also like to gratefully acknowledge useful discussions with M. Bird, R. Coehoorn, M. Gwinner, M. Kemerink, L. J. A. Koster, H. Sirringhaus, and J. Zaumseil. This work was performed using the Darwin Supercomputer of the University of Cambridge High Performance Computing Service (http://www.hpc.cam.ac.uk/), provided by Dell Inc. using Strategic Research Infrastructure Funding from the Higher Education Funding Council for England.

*cg378@cam.ac.uk

[1] M. P. Langevin, Ann. Chim. Phys. **7**, 433 (1903).
[2] R. G. Kepler and F. Coppage, Phys. Rev. **151**, 610 (1966).
[3] M. Silver and R. Sharma, J. Chem. Phys. **46**, 692 (1967).
[4] P. W. M. Blom, M. J. M. de Jong, and S. Breedijk, Appl. Phys. Lett. **71**, 930 (1997).
[5] J. Zaumseil, R. H. Friend, and H. Sirringhaus, Nature Mater. **5**, 69 (2006).
[6] J. Zaumseil, C. R. McNeill, M. Bird, D. L. Smith, P. P. Ruden, M. Roberts, M. J. McKiernan, R. H. Friend, and H. Sirringhaus, J. Appl. Phys. **103**, 064517 (2008).
[7] J. S. Swensen, J. Yuen, D. Gargas, S. K. Buratto, and A. J. Heeger, J. Appl. Phys. **102**, 013103 (2007).
[8] J. Zaumseil, C. Groves, J. M. Winfield, N. C. Greenham, and H. Sirringhaus, Adv. Funct. Mater. (to be published).
[9] L. Onsager, Phys. Rev. **54**, 554 (1938).
[10] C. L. Braun, J. Chem. Phys. **80**, 4157 (1984).
[11] R. A. Marsh, C. Groves, and N. C. Greenham, J. Appl. Phys. **101**, 083509 (2007).
[12] P. K. Watkins, A. B. Walker, and G. L. B. Verschoor, Nano Lett. **5**, 1814 (2005).
[13] T. Offermans, S. C. J. Meskers, and R. A. J. Janssen, Chem. Phys. **308**, 125 (2005).
[14] C. Groves, R. A. Marsh, and N. C. Greenham, J. Chem. Phys. **129**, 114903 (2008).
[15] U. Albrecht and H. Bässler, Chem. Phys. Lett. **235**, 389 (1995).
[16] H. Sano and M. Tachiya, J. Chem. Phys. **71**, 1276 (1979).
[17] A. Pivrikas, R. Österbacka, G. Juška, K. Arlauskas, and H. Stubb, Synth. Met. **155**, 242 (2005).
[18] G. Sliaužys, G. Juška, K. Arlauskas, A. Privikas, R. Österbaka, M. Scharber, A. Mozer, and N. C. Sariciftci, Thin Solid Films **511-512**, 224 (2006).
[19] A. Pivrikas, G. Juška, A. J. Mozer, M. Scharber, K. Arlauskas, N. S. Sariciftci, H. Stubb, and R. Österbacka, Phys. Rev. Lett. **94**, 176806 (2005).
[20] G. Juška, K. Arlauskas, J. Stuchlik, and R. Österbacka, J. Non-Cryst. Solids **352**, 1167 (2006).
[21] G. Juška, K. Arlauskas, G. Sliaužys, A. Privikas, A. J. Mozer, N. S. Sariciftci, M. Sharber, and R. Österbacka, Appl. Phys. Lett. **87**, 222110 (2005).
[22] L. J. A. Koster, V. D. Mihailetchi, and P. W. M. Blom, Appl. Phys. Lett. **88**, 052104 (2006).
[23] C. G. Shuttle, B. O'Regan, A. M. Ballantyne, J. Nelson, D. D. C. Bradley, J. de Mello, and J. R. Durrant, Appl. Phys. Lett. **92**, 093311 (2008).
[24] A. Pivrikas, N. S. Sariciftci, G. Juška, and R. Österbacka, Prog. Photovoltaics **15**, 677 (2007).
[25] N. C. Greenham and P. A. Bobbert, Phys. Rev. B **68**, 245301 (2003).
[26] I. Balberg, R. Naidis, M. K. Lee, J. Shinar, and L. F. Fonseca, Appl. Phys. Lett. **79**, 197 (2001).
[27] G. J. Adriaenssens and V. I. Arkhipov, Solid State Commun. **103**, 541 (1997).
[28] J. Nelson, S. A. Choulis, and J. R. Durrant, Thin Solid Films **451**, 508 (2004).
[29] U. Albrecht and H. Bässler, Phys. Status Solidi B **191**, 455 (1995).
[30] U. Albrecht and H. Bässler, Chem. Phys. **199**, 207 (1995).
[31] Y. N. Gartstein, E. M. Conwell, and M. J. Rice, Chem. Phys. Lett. **249**, 451 (1996).
[32] K. D. Meisel, W. F. Pasverr, J. Cotaar, C. Tanase, R. Coehoorn, P. A. Bobbert, P. W. M. Blom, D. M. de Leeuw, and M. A. J. Michels, Phys. Status Solidi C **3**, 267 (2006).
[33] R. A. Marcus, Rev. Mod. Phys. **65**, 599 (1993).
[34] J. J. Lukkien, J. P. L. Segers, P. A. J. Hilbers, R. J. Gelten, and A. P. J. Jansen, Phys. Rev. E **58**, 2598 (1998).
[35] C. R. McNeill, S. Westenhoff, C. Groves, R. H. Friend, and N. C. Greenham, J. Phys. Chem. C **111**, 19153 (2007).
[36] E. C. P. Smits, T. D. Anthopoulos, S. Setayesh, E. van Veenendaal, R. Coehoorn, P. W. M. Blom, B. de Boer, and D. M. de Leeuw, Phys. Rev. B **73**, 205316 (2006).
[37] M. Kemerink, D. S. H. Charrier, E. C. P. Smits, S. G. J. Mathijssen, D. M. de Leeuw, and R. A. J. Janssen, Appl. Phys. Lett. **93**, 033312 (2008).
[38] I. Jurić, I. Batistić, and E. Tutiš, Phys. Rev. B **77**, 165304 (2008).
[39] R. C. G. Naber, M. Bird, and H. Sirringhaus, Appl. Phys. Lett. **93**, 023301 (2008).
[40] We can provide a rough estimate of the effect of alignment by assuming that alignment increases the mobility and the current along the channel by a factor of A compared to the unaligned case, and that the mobility in the perpendicular directions remains unchanged. Reference 36 shows that $W \propto \frac{1}{\sqrt{\Phi}}$, where Φ is the factor change in the recombination rate. Consequently, Eq. (3) predicts that alignment will increase W by a factor of $A^{0.25}$ and thus the exciton density will increase by $A^{0.75}$. Therefore to yield the factor of 10^3 improvement in exciton density required, A must be at least 10^4, which seems very unlikely to be realized in reality. Furthermore, these assumptions are a best-case scenario, and in reality the current will increase by less than a factor of A due to the frequent interchain hops required to traverse the channel.